

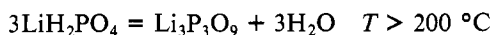
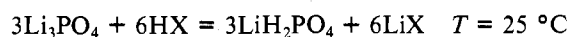
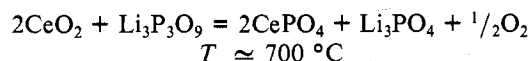
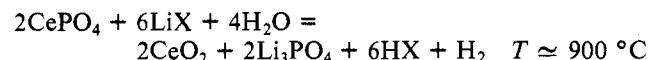
fact that evaporation of H<sub>2</sub>O from solutions containing LiX's and H<sub>3</sub>PO<sub>4</sub> gives rise to steam volatilization of H<sub>3</sub>PO<sub>4</sub>, and some back-reaction of H<sub>3</sub>PO<sub>4</sub> with the crystallized LiX's to produce HX and lithium phosphates.

In a typical ion-exchange experiment, 9.9 mmol (29.7 mequiv) of Li<sub>3</sub>PO<sub>4</sub> was slurried in water with 8.09 g (20.1 mequiv) of acid-treated Dowex 50W ion-exchange resin. The mixture was filtered, and titration of the resulting solution showed that it contained 1.1 mmol (3.3 mequiv) of H<sub>3</sub>PO<sub>4</sub> and 8.2 mmol (16.4 mequiv) of H<sub>2</sub>PO<sub>4</sub><sup>-</sup>. Therefore, the total dissolved phosphate was 9.3 mmol or 94% of that originally used; 19.7 mequiv of acid was consumed or 98% of that originally used. The Li<sup>+</sup> was then eluted from the resin with excess 1 N HCl; subsequent titration of the acid in the combined eluant solutions showed that 18.8 mequiv of HCl remained on the column, an amount equivalent to 95.4% of the 19.7 mequiv of Li which was adsorbed.

In other experiments, mixtures of CeO<sub>2</sub> and Li<sub>3</sub>PO<sub>4</sub> produced from reaction 1 were treated with excess 1 N HCl to dissolve all of the Li<sub>3</sub>PO<sub>4</sub>. The solution was collected by centrifugation and passed through an acid-treated Dowex 50W column. Titration of the eluant solutions showed that 100.0 ± 0.7% of the Li<sub>3</sub>PO<sub>4</sub> had been converted to H<sub>3</sub>PO<sub>4</sub>. The Li<sup>+</sup> was then eluted from the resin in the manner described above.

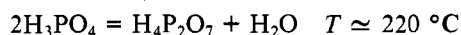
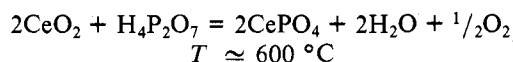
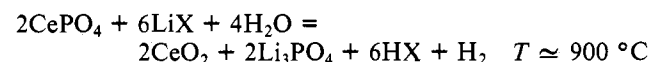
The solid products of reaction 1 can be separated prior to treatment with HX by flotation in 1,1,2,2-tetrabromoethylene, but only if the solids are slurried in water first. An H<sub>2</sub>O-Li<sub>3</sub>PO<sub>4</sub> suspension floats on the Br<sub>2</sub>CHCHBr<sub>2</sub>(l); CeO<sub>2</sub>(s) is more dense and sinks to the bottom of the system. In typical experiments, a single treatment yielded a lighter aqueous suspension containing 89% of the Li<sub>3</sub>PO<sub>4</sub> and a solid containing all of the CeO<sub>2</sub> and the remainder of the Li<sub>3</sub>PO<sub>4</sub>.

**E. Summary. Combination of These Reactions into Thermochemical Cycles.** Reactions 1, 8-11, and those described in section D can be combined into at least two types of thermochemical cycles. Cycle 1 (separation steps are not Cycle 1



shown) combines eq 1 with eqs 8 and 9 and the acidification of Li<sub>3</sub>PO<sub>4</sub>. Note that the sum of all the reactions is just H<sub>2</sub>O = H<sub>2</sub> + 1/2 O<sub>2</sub>. In Cycle 2, eq 1 is combined with eq 10 and

Cycle 2



11 and the acidification of Li<sub>3</sub>PO<sub>4</sub>. The maximum required temperature is the same for both cycles. Cycle 2 is simpler and requires less phosphate, but Cycle 1 avoids the potential problems of dealing with H<sub>3</sub>PO<sub>4</sub> at high temperatures. The practicality of both cycles is minimized by need to use an ion-exchange resin for a separation step.

### Experimental Section

**A. Reagents.** CeO<sub>2</sub> (99.9% pure) was purchased from Gallard-Schlesinger. "Certified" LiOH·H<sub>2</sub>O, LiBr·H<sub>2</sub>O, and LiCl were from

Fisher Chemical. LiI·3H<sub>2</sub>O ("purified") was from City Chemical Corp., N.Y. Reagent grade Li<sub>2</sub>CO<sub>3</sub> came from Allied Chemical. "AR" grade H<sub>3</sub>PO<sub>4</sub> (85%) was purchased from Mallinckrodt. Dowex 50W-X8 was obtained from Bio-Rad Laboratories, and 1,1,1,3,3-tetrabromoethane was from Mallinckrodt.

Li<sub>3</sub>PO<sub>4</sub> was prepared by mixing LiOH·H<sub>2</sub>O with a stoichiometric amount of 85% H<sub>3</sub>PO<sub>4</sub>. The resulting Li<sub>3</sub>PO<sub>4</sub> was washed several times with deionized water and fired in a platinum dish to 500 °C. It was analyzed by titration with HCl, which showed the solid to be Li<sub>3</sub>PO<sub>4</sub>·0.02H<sub>2</sub>O (EW = 38.73 g).

CePO<sub>4</sub> was prepared by reducing CeO<sub>2</sub> with 47% HI (Mallinckrodt). The resulting solution was filtered and then treated with excess H<sub>3</sub>PO<sub>4</sub> (85%). Impure CePO<sub>4</sub> precipitated. This was collected by filtration and purified three times by boiling an aqueous suspension of the solid for 1 h. The purified product was analyzed by X-ray powder diffraction<sup>5</sup> and by neutron activation analysis.

**B. High-Temperature Experiments.** In these experiments, the solid reactants were ground together and placed into a platinum boat, which was covered with Pt foil and introduced into a fused-quartz tube. A tube furnace was then used to heat the solids. A continuously flowing stream of Ar at essentially 1 atm pressure was used to purge air from the tube and to carry evolved gases away from the solids and into calibrated, continuously operating measurement devices—a Gow-Mac Model 20-150 thermal conductivity detector for H<sub>2</sub> and a Beckman Model 741 oxygen analyzer. Steam was preheated to 220 °C and passed over the Pt boat at a rate equivalent to 3.2-4.8 mL of condensed H<sub>2</sub>O(l)/min. For reactions involving LiX's, the resulting HX was condensed with the steam from the Ar stream by a water-cooled condenser. The amounts of evolved HX were determined by titration with standardized NaOH. For reactions involving Li<sub>2</sub>CO<sub>3</sub>, the resulting CO<sub>2</sub>(g) was trapped in a solution of 2 N NaOH. In every case, a CaSO<sub>4</sub> column was used to dry the Ar-H<sub>2</sub> or Ar-O<sub>2</sub> mixtures before they reached the gas-measuring devices.

A thermal controller was used to increase the reaction temperatures at a steady rate, usually about 5 °C/min. Solid products were characterized by X-ray powder diffraction<sup>5</sup> and by acid-base titration.

**Acknowledgment.** Research was sponsored by the Division of Chemical Sciences, Office of Basic Energy Sciences, U.S. Department of Energy, under Contract W-7405-eng-26 with Union Carbide Corp.

**Registry No.** CePO<sub>4</sub>, 13454-71-2; LiCl, 7447-41-8; LiBr, 7550-35-8; LiI, 10377-51-2; H<sub>2</sub>O, 7732-18-5.

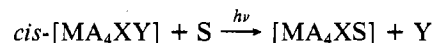
Contribution from the Department of Chemistry, Kansas State University, Manhattan, Kansas 66506

### Theoretical Prediction and Experimental Confirmation of Trans to Cis Photoisomerization in d<sup>6</sup> Transition-Metal Complexes

Keith F. Purcell,\* Stephen F. Clark,<sup>†</sup> and John D. Petersen\*<sup>†</sup>

Received November 28, 1979

Experimental study of photosubstitution reactions



has led to the generalization that geometrical isomerization is often expected when M = d<sup>6</sup> metal ion. The reasons for this recently have been given by Vanquickenborne and Ceulemans (V/C) in an angular overlap model (AOM) study.<sup>1</sup> Prior to their report, one of us had already discovered (and subsequently published<sup>2</sup>) that *cis*-[Rh(en)<sub>2</sub>(NH<sub>3</sub>)Cl]<sup>2+</sup> did not fit the generalization, and we embarked on an AOM study of our own. Where they overlap, our independent calculations

<sup>†</sup>Current address is Department of Chemistry, Clemson University, Clemson, SC 29631.

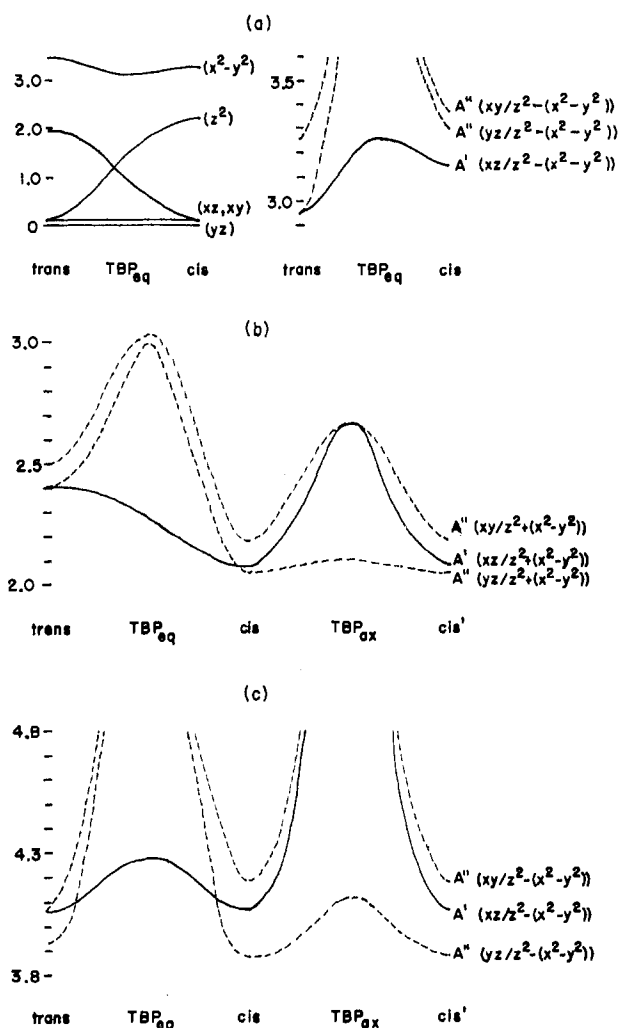


**Figure 1.** Orbital and triplet-state correlations for the  $\text{trans} \rightleftharpoons \text{cis}$  and  $\text{cis} \rightleftharpoons \text{cis}'$  isomerization reactions of  $[\text{MA}_4\text{X}]$ . The transition-state structures are trigonal bipyramids for both isomerization reactions, but they differ in that X is equatorial for  $\text{trans} \rightleftharpoons \text{cis}$  and axial for  $\text{cis} \rightleftharpoons \text{cis}'$ . Energies are in  $\mu\text{m}^{-1}$  units. The orbital labels are those appropriate to the coordinate system given in the text for the cis structure with  $A_2$  on the  $+y$  axis; under  $C_s$  symmetry the  $(z^2)$  and  $(x^2 - y^2)$  orbitals are mixed. The  $A'$  state is dominated by the configuration  $(xy)^2(yz)^2(xz)^1(z^2)^1$  while the  $A''$  states are dominated by  $(xy)^2(yz)^1(xz)^2(z^2)^1$  and  $(xy)^1(yz)^2(xz)^2(z^2)^1$ , in order of increasing energy: (a) the case discussed by V/C, ( $e_\sigma^A = 1.16$ ,  $e_\pi^A = 0.0$ ) and ( $e_\sigma^X = 0.83$ ,  $e_\pi^X = 0.1$ ); (b) an example of  $\text{trans} \rightarrow \text{cis}$ , ( $e_\sigma^A = 0.5$ ,  $e_\pi^A = 0.0$ ) and ( $e_\sigma^X = 1.0$ ,  $e_\pi^X = 0.1$ ); (c) an example of  $A''$  below  $A'$  due to orbital energies, ( $e_\sigma^A = 1.16$ ,  $e_\pi^A = 0.1$ ) and ( $e_\sigma^X = 1.11$ ,  $e_\pi^X = -0.1$ ).

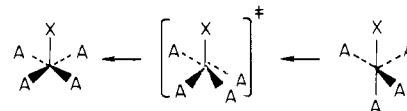
confirm those of V/C (see Figure 1a, for an example). However, we did examine the phenomenon in a broader scope and wish to comment on two predictions not considered by V/C and present the experimental verification of one of these predictions.

### Results and Discussion

We begin with a brief recounting of the V/C conclusions:

(1) Photosubstitution of  $[\text{MA}_4\text{XY}]$  occurs by loss of Y in the lowest triplet state.

(2) With use of cis and trans to denote the positions of X and the vacant site, it is found that *cis*- and *trans*- $[\text{MA}_4\text{X}]$  are separated by an often low-activation barrier at the trigonal-bipyramidal structure.



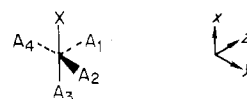
(3) When X is a poorer  $\sigma$  donor than A (and M–ligand  $\pi$  bonding is minimal), the *trans* structure is favored and the barrier to *cis* to *trans* isomerization is low in relation to the triplet  $\rightarrow$  singlet deactivation rate constant; thermodynamic control of product structures is expected and generally found.

Our work enables us to concur with these conclusions but also to predict (1) that the  $\text{trans} \rightarrow \text{cis}$  isomerization is expected when X is a better  $\sigma$  donor than A and (2) that photoracemization is possible for certain A,X combinations.

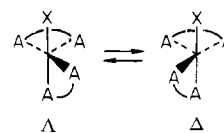
Figure 1b is shown to illustrate that as  $e_\sigma^X$  approaches  $2e_\sigma^A$ , the barrier between *trans*- and *cis*- $\text{MA}_4\text{X}$  disappears, with *cis* thermodynamically favored and *trans* becoming a transition-state structure for the (stereoretentive for chelates) rearrangement.

For confirmation of this *trans* to *cis* isomerization, we studied the ligand field photolysis of *trans*- $\text{Co}(\text{en})_2(\text{CN})\text{Cl}^+$  and *trans*- $\text{Co}(\text{en})_2(\text{CN})\text{H}_2\text{O}^{2+}$ . Our choice of Co(III) as the metal center was made in order to reduce the absolute values of  $e_\sigma$  and  $e_\pi$  and allow thermodynamic and not kinetic control of products. Loss of  $\text{Cl}^-$  from the former complex ( $\phi = 1.6 \times 10^{-2}$  mol/einstein) and  $\text{H}_2\text{O}$  from the latter complex ( $\phi = 2.5 \times 10^{-2}$  mol/einstein) leads to the same  $\text{Co}(\text{en})_2(\text{CN})^{2+}$  ( $\text{CN}^-$  *trans* to vacant site) intermediate. Carbon-13 NMR spectroscopy confirms that the photolysis product in both cases is *cis*- $\text{Co}(\text{en})_2(\text{CN})(\text{H}_2\text{O})^{2+}$ . These experimental results confirm the AOM prediction and strengthen the arguments favoring excited-state vs. "hot" ground-state reactivity in  $d^6$  photosubstitution reactions since the electronic configuration of the ligand field excited state is maintained after ligand loss.<sup>3</sup>

Figure 1b raises a second point of interest. Note in this instance, and others as well, the crossing of the  ${}^3A'$  and  ${}^3A''$  states near the *cis* structure. The principal contributors to these states are the configurations  $({}^3A') (xy)^2(yz)^2(xz)^1(z^2)^1$  and  $({}^3A'') (xy)^2(yz)^1(xz)^2(z^2)^1$ .



As noted by V/C, motion of  $(A_1, A_3)$  in the  $xz$  plane (to give the TBP with X equatorial) is favored over motion of  $(A_2, A_4)$  in the  $yz$  plane (to give the TBP with X axial) for the  ${}^3A'$  configuration. This is due to destabilization of  $(xz)$ , occupied by only one electron, in the former case, compared to destabilization of  $(yz)$ , occupied by two electrons, in the latter. We noted, by analogy, that  $(A_2, A_4)$  motion should be favored for the  ${}^3A''$  state. Now,  $(A_2, A_4)$  motion will lead to racemization of  $[\text{M}(\text{A}-\text{A})_2\text{X}]$  species:



so one might expect to find photoracemization occurring when the *cis* complex is prepared in the  ${}^3A''$  state or when prepared in  ${}^3A'$ , but a crossing of  ${}^3A'$  and  ${}^3A''$  occurs at low energy. As shown in Figure 1b, photoracemization is a distinct possibility for cases where *trans* to *cis* is spontaneous and uninhibited, starting from the *trans* form and from the *cis* form. (The

(1) Vanquickenborne, L. G.; Ceulemans, A. *Inorg. Chem.* **1978**, *17*, 2730.  
(2) Petersen, J. D.; Jakse, F. P. *Inorg. Chem.* **1979**, *18*, 1818.

(3) As fate would have it, while this paper was in preparation Ford and Skibsted published the first example of *trans* to *cis* isomerization: *J. Chem. Soc., Chem. Commun.* **1979**, 853.

zero-order AOM orbital energies can be used to show that the trans  $\rightarrow$  cis barrier on  ${}^3A'$  should be nearly the same as the  $\Lambda \rightleftharpoons \Delta$  barrier on  ${}^3A''$ .)

Both  $\sigma$  and  $\pi$  ligand properties may be selected to cause a low lying  ${}^3A''$  state and photoracemization. Figure 1c illustrates the effect of  $e_{\pi}^A > e_{\pi}^X$  ( $A$  is a  $\pi$  donor and  $X$  is a  $\pi$  acceptor). The  $\sigma$  effect arises from  $(z^2)/(x^2 - y^2)$  mixing and electron-repulsion energies.  $e_{\sigma}^X \neq e_{\sigma}^A$  is required for  $(z^2)/(x^2 - y^2)$  mixing; the perturbed  $(z^2)$  MO, which always lies lower than the  $(x^2 - y^2)$  MO, has the form  $(z^2) + \lambda(x^2 - y^2)$ . As  $\lambda < \text{or} > 0$  the  $(z^2)$  torus becomes ellipsoidal, with the major axis along the  $y$  or  $x$  axis, respectively. Thus  $\lambda > 0$  results in less electron repulsion for the  ${}^3A''$  than  ${}^3A'$  state. First-order perturbation theory may be used to show that  $\lambda > 0$  whenever the off-diagonal Hamiltonian element between  $(z^2)$  and  $(x^2 - y^2)$  is negative. This requirement is met whenever  $e_{\sigma}^X > e_{\sigma}^A$ , as in Figure 1b (note that the  $\sigma$  effect overrides the fact that  $e_{\pi}^X > e_{\pi}^A$  in this case).

### Theoretical Methods

The computational technique used is the same as that used by V/C, by one of us previously,<sup>4</sup> and by others.<sup>5</sup> In short, the AOM approximation to the full, one-electron Hamiltonian matrix is established for structures along the reaction coordinate, in a basis of metal  $d$  and ligand  $\sigma$  and  $\pi$  orbitals. Diagonalization of this matrix produces a basis of one-electron MO's and energies. The latter serve as a basis for construction of Slater determinants for all  $d^6$  configurations possible. This basis is made diagonal under the  $S^2$  operator, and a full CI calculation is performed with Racah  $B$  and  $C$  parameters to include state mixing by electron repulsion forces. The results are presented in terms of orbital and state correlation diagrams.

As the purpose of this study was limited to investigation of relative  $A$  and  $X$   $\sigma$ - and  $\pi$ -bonding effects on the triplet-state surface characteristics, we have utilized a range of the AOM  $e_{\sigma}$  and  $e_{\pi}$  parameters so as to encompass a variety of  $M/A/X$  combinations. These values (in  $\mu\text{m}^{-1}$ ) are  $(0.5 \leq e_{\sigma}^A \leq 1.16)$ ,  $(0 \leq e_{\pi}^A \leq 0.1)$ ,  $(0.5 \leq e_{\sigma}^X \leq 1.16)$ , and  $(-0.1 \leq e_{\pi}^X \leq 0.1)$ . These values include those of V/C for  $\text{NH}_3$  ( $e_{\sigma} = 1.14$ ,  $e_{\pi} = 0$ ) and for  $\text{Cl}^-$  ( $e_{\sigma} = 0.86$ ,  $e_{\pi} = 0.14$ ). The nominal values for  $B$  and  $C$  of 0.035 and 0.14, respectively, were used.<sup>6</sup>

### Experimental Methods

The *trans*-[Co(en)<sub>2</sub>(CN)Cl]Cl complex was prepared by a previously reported procedure.<sup>7</sup> The *trans*-[Co(en)<sub>2</sub>(CN)(H<sub>2</sub>O)<sup>2+</sup> ion was prepared by the addition of perchloric acid to *trans*-[Co(en)<sub>2</sub>(CN)(OH)]Cl.<sup>7</sup> The stereochemistry of the *cis*-[Co(en)<sub>2</sub>(CN)(H<sub>2</sub>O)]<sup>2+</sup> photolysis product was confirmed by electronic absorption spectroscopy<sup>8</sup> and <sup>13</sup>C NMR spectroscopy by using techniques previously described.<sup>9,10</sup> The *trans* starting materials show only one carbon peak in the ethylenediamine region, while the *cis* product shows four nonequivalent ethylenediamine carbon atoms.

Photolysis reactions utilized the 488-nm (1.5-W) line of a Spectra-Physics argon-ion laser and procedures previously described.<sup>11</sup> Usable light intensities were determined by using Reineckate actinometry.<sup>12</sup>

**Acknowledgment.** This work was supported by NSF and also acknowledgment is made to the donors of the Petroleum Research Fund, administered by the American Chemical Society, for partial support (K.F.P.).

**Registry No.** *trans*-Co(en)<sub>2</sub>(CN)Cl<sup>+</sup>, 51321-29-0; *trans*-Co(en)<sub>2</sub>(CN)(H<sub>2</sub>O)<sup>2+</sup>, 19414-12-1; *cis*-Co(en)<sub>2</sub>(CN)(H<sub>2</sub>O)<sup>2+</sup>, 45978-53-8.

Contribution from the Department of Chemistry, University of New Mexico, Albuquerque, New Mexico 87131

### The 254-nm Photochemistry of the Rhodo Chromium(III) Complex: Observation of New Photosubstitution Reactions

R. R. Ruminski and W. F. Coleman\*

Received November 6, 1979

The thermal reactions of the binuclear rhodo chromium(III) complex [Cr(NH<sub>3</sub>)<sub>5</sub>OHCr(NH<sub>3</sub>)<sub>5</sub>]<sup>5+</sup> and the related aquo erythro [Cr(NH<sub>3</sub>)<sub>5</sub>OHCr(NH<sub>3</sub>)<sub>4</sub>OH<sub>2</sub>]<sup>5+</sup> and chloro erythro [Cr(NH<sub>3</sub>)<sub>5</sub>OHCr(NH<sub>3</sub>)<sub>4</sub>Cl]<sup>4+</sup> complexes have been extensively investigated.<sup>1,2</sup> In acidic solution the bridge in the rhodo ion is cleaved to produce Cr(NH<sub>3</sub>)<sub>5</sub>OH<sub>2</sub><sup>3+</sup> in HClO<sub>4</sub> and Cr(NH<sub>3</sub>)<sub>5</sub>OH<sub>2</sub><sup>3+</sup> together with Cr(NH<sub>3</sub>)<sub>5</sub>Cl<sup>2+</sup> in HCl.

The photochemical reactions of the aquo and chloro erythro complexes, following excitation into the two lowest lying quartet excited states, traditionally labeled L<sub>1</sub> and L<sub>2</sub>, have also been reported.<sup>3</sup> The photochemical reactions that were observed consisted solely of ligand substitution and isomerization processes that retained the binuclear structure of the initial complexes. Once the data were corrected for the thermal reaction, no bridge-cleavage products were obtained. We have recently studied the ligand field photochemistry of the rhodo complex in a variety of acid media.<sup>4</sup> Our findings parallel those obtained in ref 3 for the erythro complexes. No bridge cleavage is observed when the rhodo complex is excited into L<sub>1</sub> and L<sub>2</sub> over the temperature range 5–35 °C.

We report here a study of the 254-nm photochemistry of the rhodo ion in aqueous acid media and the observation of photoinduced bridge cleavage.

### Experimental Section

The rhodo complex was prepared as the chloride salt according to the method of Linhard and Weigel.<sup>5</sup> Anal. Calcd for [Cr(NH<sub>3</sub>)<sub>5</sub>OHCr(NH<sub>3</sub>)<sub>5</sub>]Cl<sub>5</sub>·*n*H<sub>2</sub>O: mole ratio N/Cr = 5.00. Found: mole ratio N/Cr = 5.00. The chloride salt was converted to solutions of the nitrate and perchlorate salts by the addition of AgNO<sub>3</sub> and AgClO<sub>4</sub>, respectively. The precipitated AgCl was removed by filtration. Subsequent tests showed no evidence of residual Ag<sup>+</sup> or Cl<sup>-</sup> in the solutions. The absorption spectra and extinction coefficients of the rhodo ion were independent of the anion, in the L<sub>1</sub> and L<sub>2</sub> bands, and were in quantitative agreement with those published previously.<sup>1,6</sup>

Solutions were photolyzed in a Rayonet Model RPR-100 photochemical reactor equipped with 12 Rayonet RPR 1849-Å/2537-Å lamps. The output of these lamps is concentrated (>95% of the light into the cell) in the 254-nm Hg line. The solutions were contained in a thermostated, jacketed quartz photolysis cell which can be stirred during photolysis and purged with gas. In some experiments the solutions were put through several freeze-thaw cycles prior to irradiation and purged with N<sub>2</sub> during photolysis. Temperature control was good to  $\pm 1$  °C.

Reaction products were ion exchanged by using Sephadex C-25 cation-exchange resin. The various cationic species were eluted with

- (4) Purcell, K. F. *J. Am. Chem. Soc.* **1979**, *101*, 5147.
- (5) Burdett, J. K. *Inorg. Chem.* **1976**, *15*, 212. Lohr, L. L., Jr.; Grimmeimann E. I. *J. Am. Chem. Soc.* **1978**, *100*, 1100. Schaffer, C. E.; Jorgensen, E. K. *Mol. Phys.* **1965**, *9*, 401. Schaffer, C. E. *Struct. Bonding (Berlin)* **1968**, *5*, 68.
- (6) König, E.; Schnäkig, R. *Inorg. Chim. Acta* **1973**, *7*, 383.
- (7) Chan, S. C.; Tobe, M. L. *J. Chem. Soc.* **1963**, 966.
- (8) Ohkawa, K.; Hidaka, J.; Shimura, Y. *Bull. Chem. Soc. Jpn.* **1967**, *40*, 2830.
- (9) Jakse, F. P.; Paukstelis, J. V.; Petersen, J. D. *Inorg. Chim. Acta* **1978**, *27*, 225.
- (10) House, D. A.; Blunt, J. W. *Inorg. Nucl. Chem. Lett.* **1975**, *11*, 219.
- (11) Figard, J. E.; Petersen, J. D. *Inorg. Chem.* **1978**, *17*, 1059.
- (12) Wegner, E. E.; Adamson, A. W. *J. Am. Chem. Soc.* **1966**, *88*, 394.

- (1) D. W. Hoppenjans and J. B. Hunt, *Inorg. Chem.*, **8**, 505 (1969).
- (2) C. S. Garner and D. A. House, *Transition Met. Chem.*, **6**, 59 (1970).
- (3) P. Ricceri and E. Zinato, *Inorg. Chim. Acta*, **7**, 117 (1973).
- (4) R. R. Ruminski, M.S. Thesis, University of New Mexico, 1977.
- (5) M. Linhard and M. Weigel, *Z. Anorg. Allg. Chem.*, **299**, 15 (1959).
- (6) L. Dubicki and R. L. Martin, *Aust. J. Chem.*, **23**, 215 (1970).